

Introduction

Seismic-wave modelling including temperature is an improved tool for the geophysical characterization of deep structures in geothermal and volcanic-caldera areas. We study two target Mexican geothermal fields: the Los Humeros superhot-geothermal system (SHGS) and the Acoculco potential enhanced-geothermal system (EGS). The study covers analytical aspects and full-waveform signal simulation in poro-viscoelastic formation including possible melting conditions in the proximity of the brittle-ductile transition (BDT) characterized by rock thermodynamic Arrhenius parameters and temperature, as well as pressure and fluid-phase properties. The analysis includes possible supercritical conditions, and different hydrothermal mechanisms, by convective and conductive heat transport (see also GEMex Deliverable 5.5, Poletto et. al, 2019a).

Burgers-Gassmann mechanical model

The utilized full-wave solver (Carcione et al., 2017) is based on the Burgers mechanical model, which allows us to describe the anelastic behavior due to shear deformation and plastic flow, and the Gassmann equation to account for the fluid properties in the poro-viscoelastic model.

The shear viscosity (η) is related to the steady-state creep rate ($\dot{\epsilon}$) and the octahedral stress (σ_o) through the Arrhenius equation. The dislocation creep rate is represented by the steady state power law

$$\dot{\epsilon} = A \sigma_o^n \exp(-E/RT),$$

being A ($\text{MPa}^{-n} \text{s}^{-1}$) a material constant, n the stress exponent, E the activation energy (kJ/mole), R the gas constant and T the absolute temperature.

The saturated-rock Gassmann-Burgers bulk (K_G) and shear moduli (μ_G) are related to the dry-rock and solid matrix moduli, the porosity (ϕ) and the geothermal fluid bulk modulus. The dry-rock moduli can be related to the differential pressure (difference between the confining lithostatic pressure and the pore hydrostatic pressure) through an exponential law (Carcione et al., 2017).

The saturated-rock complex compressional and shear velocities are

$$V_{CP} = \sqrt{\frac{K_G + \frac{4}{3}\mu_G(\omega)}{\bar{\rho}}}, \quad V_{CS} = \sqrt{\frac{\mu_G(\omega)}{\bar{\rho}}}, \quad \bar{\rho} = (1 - \phi)\rho_s + \phi\rho_f,$$

where $\bar{\rho}$, ρ_s , ρ_f are the saturated-formation, the solid-matrix and the fluid densities, respectively.

The phase velocities and the quality factors are,

$$V_{P,S} = \left[\text{Re} \left(\frac{1}{V_{CP,S}} \right) \right]^{-1} \quad \text{and} \quad Q_{P,S} = \frac{\text{Re}(V_{CP,S}^2)}{\text{Im}(V_{CP,S}^2)}.$$

Sensitivity analysis

To understand the sensitivity of seismic-wave propagation to temperature and pressure variations, we performed a sensitivity analysis at low seismic frequencies assuming a temperature gradient of 90°C/km in a uniform formation using rock and geothermal parameters from reference literature (Poletto et al., 2018). In Fig. 1 we compare different behaviors in the compressional V_P (a) and shear V_S (b) phase velocities responses, in the cases of dry ($\phi = 0$) and saturated ($\phi = 5\%$) formation without and with pressure effects. Figure 2 shows the sensitivity curves (absolute value) for V_P (a) and V_S (b), without and with porosity and pressure effects. The arrows indicate the zones in which the different effects are more relevant for the sensitivity.

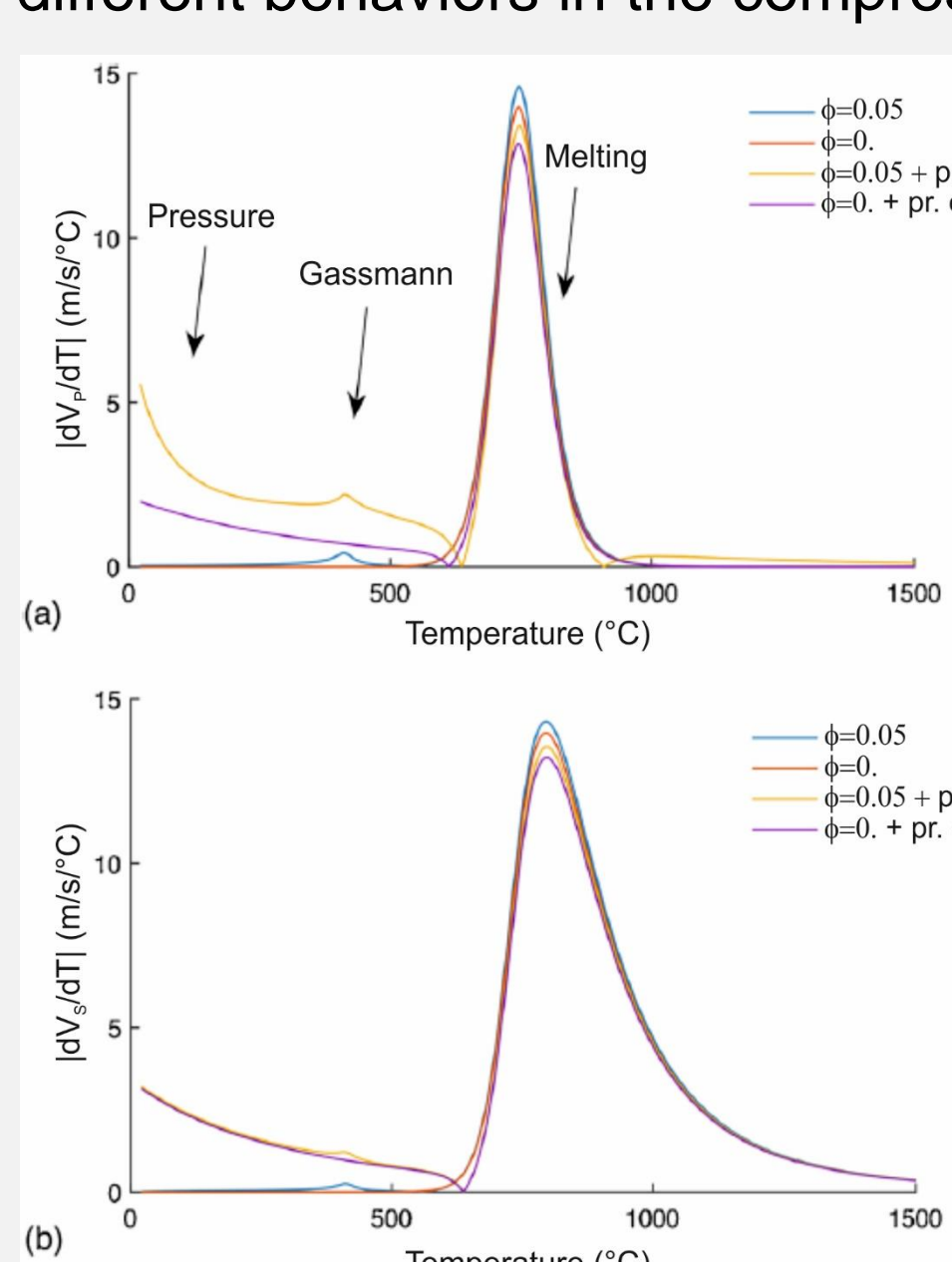


Fig. 2 Sensitivity curves for (a) V_P and (b) V_S with and without porosity and pressure effects. The arrows indicate the zones in which the different effects are more relevant for the sensitivity.

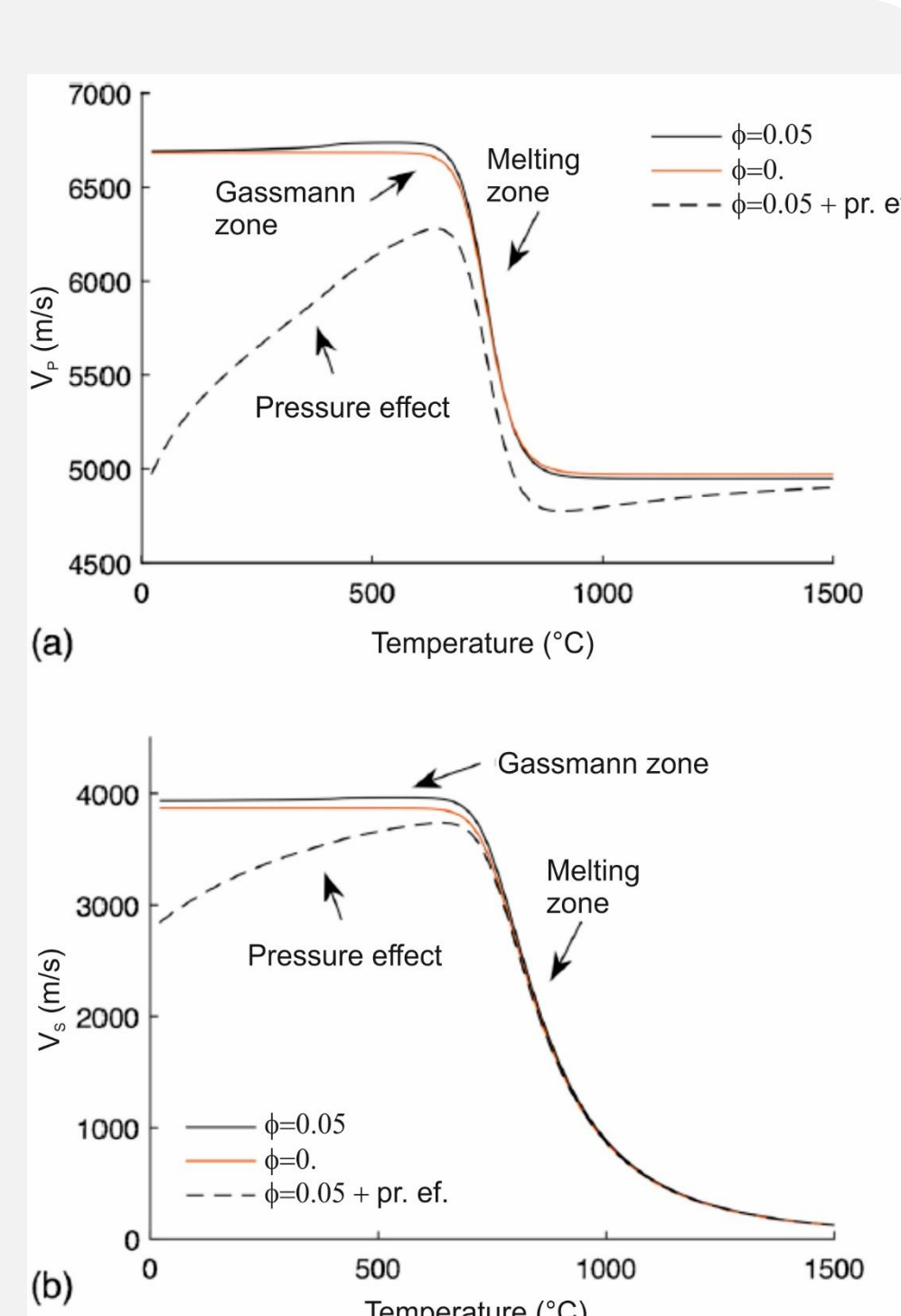


Fig. 1 (a) P-wave and (b) S-wave phase velocities calculated with and without porosity and pressure effects.

The study results show that in deeper zones the main expected contributions in terms of variations in seismic quantities due to temperature come from melting transition, while in shallower porous fluid-saturated formations the trends are governed by pressure effects.

Conductive and convective geothermal systems

We calculate the seismic properties in terms of the differential pressures and temperature distributions, assuming that the heat transfer from below is convective or conductive considering 1D temperature and petrophysical models (Farina et al., 2019).

Los Humeros SHGS

For the Los Humeros SHGS we consider possible conductive and convective heat-flow corresponding to the pressure and temperature 1D models shown in Fig. 3.

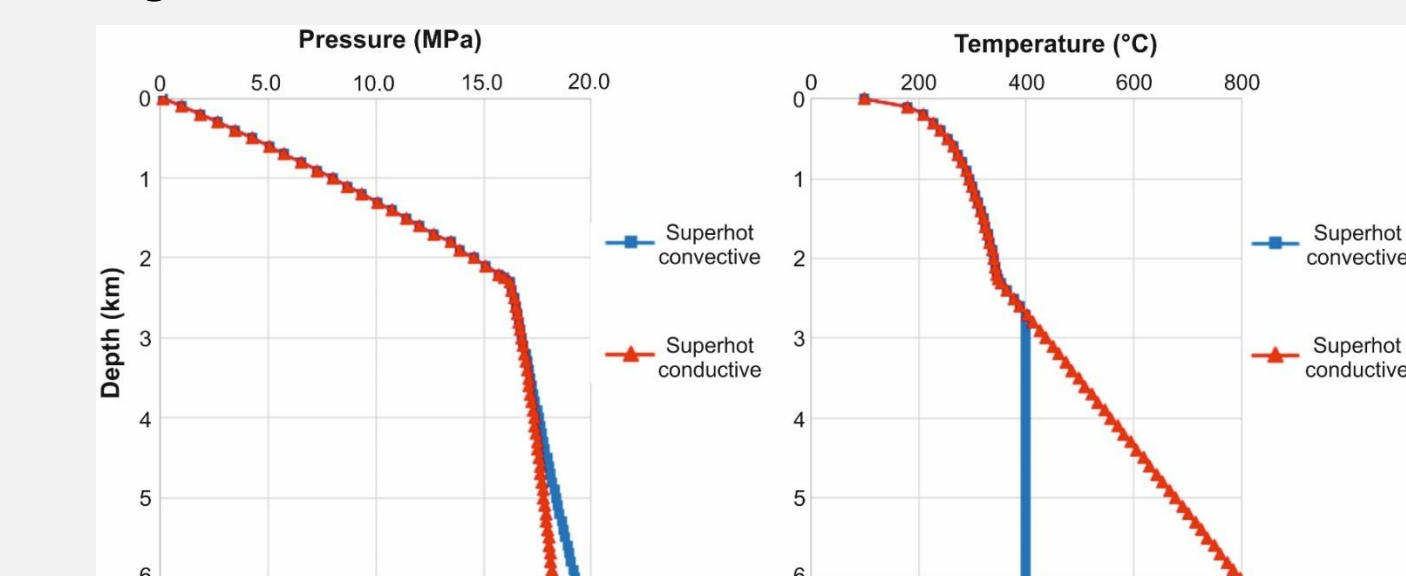


Fig. 3 Pressure and temperature profiles with convective (blue) and conductive (red) mechanism in the deeper part.

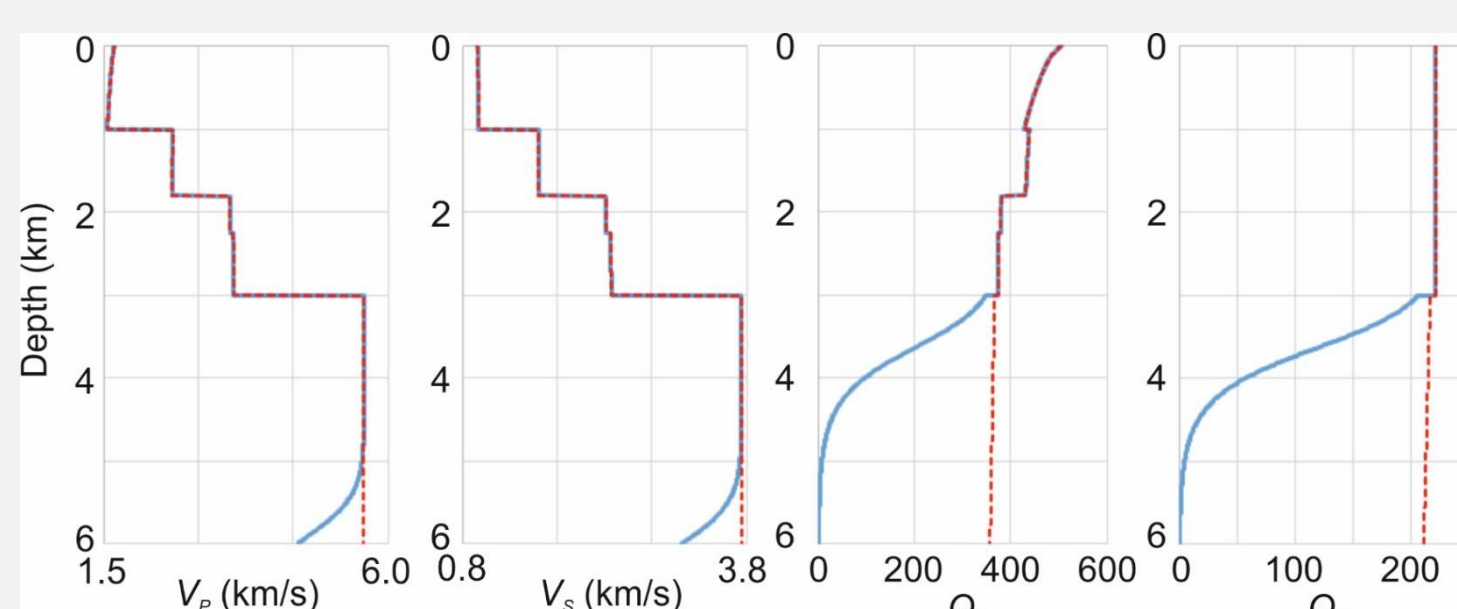


Fig. 4 P- and S-wave phase velocities and attenuations versus temperature with convective (blue) and conductive (red) models.

The 1D geological model is composed of four units (Gutiérrez and Montalvo, 2010). To evaluate the seismic response assuming the proximity of a magma chamber as a possible scenario, in the deepest unit, below 5 km depth, we use a set of Arrhenius parameters that allows rock to melt at about 700 °C. Velocity trends are shown in Fig. 4.

The decrease of seismic velocities and attenuation (Q factor) is observable only in the hypothesis of conductive heat-transport mechanism.

Acoculco EGS

For the Acoculco geothermal system we use the conductive heat-transport mechanism. Temperature and pressure profiles are shown in Fig. 5.

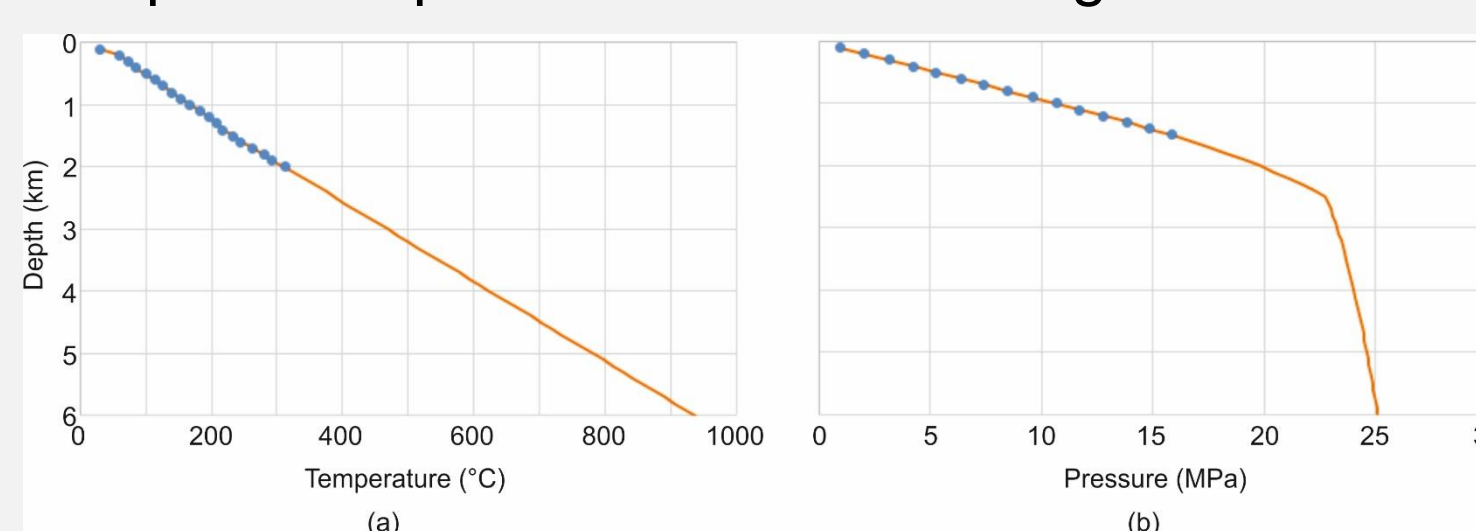


Fig. 5 (a) Temperature of well EAC-1 (blue bullets) obtained from Pulido et al. (2010) and extension to deeper depths using the geothermal gradient of 156 °C/km (orange line). (b) Pressure of well EAC-1 (blue bullets) and extension using the hydrostatic pore pressure associated to the chosen temperature gradient.

For the geological model, we consider a simplified 1D model with the main four lithological units penetrated by well EAC-1 (López-Hernández et al., 2009). In the deepest layer we assume two sets of Arrhenius parameters corresponding to two different rock behaviors at high temperature, namely AC1 for rock that melts at $T > 900^\circ\text{C}$ and AC2 for rock that melts at $T \sim 700^\circ\text{C}$.

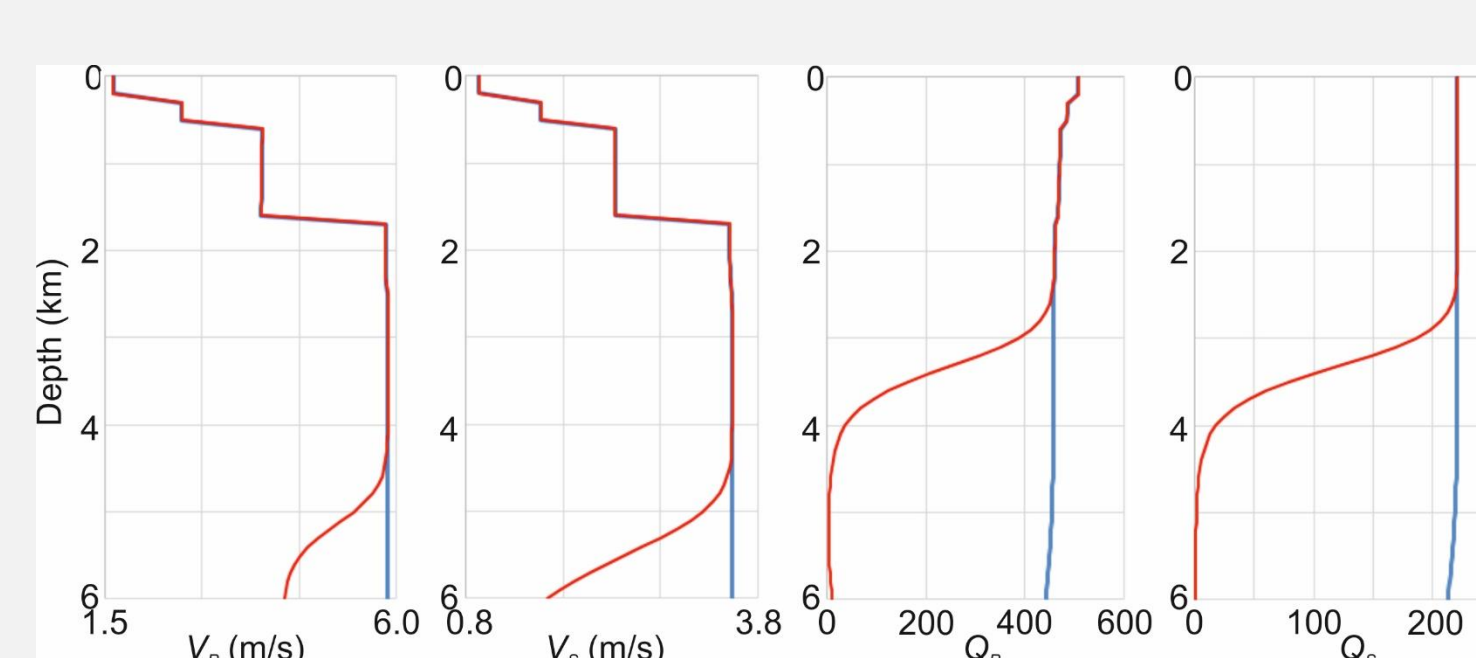


Fig. 6 P- and S-wave phase velocities and attenuations versus temperature with the last layer characterized by the Arrhenius sets AC1 (blue line) and AC2 (red line).

Simulation of Los Humeros SHGS wavefields

Los Humeros is the largest active caldera located in the northernmost part of the eastern sector of the Trans-Mexican volcanic belt. To calculate the synthetic propagation we consider the geological and temperature model (Fig. 7) proposed by Verma et al. (1990), a magma chamber under the caldera, with two cylindrical chimneys at the top of the granite unit.

We analyze two geothermal scenarios: the proximity to melting formations and the presence of superhot chimneys (Poletto et. al, 2019b).

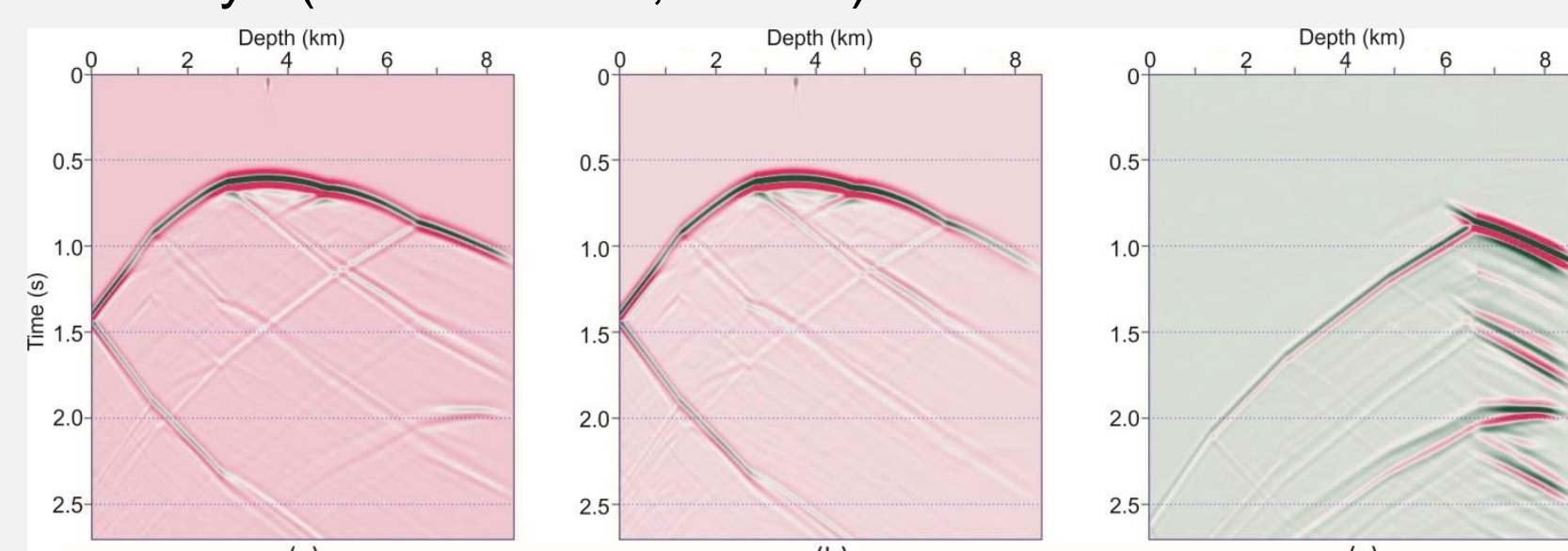


Fig. 8 Pressure-wave component of the vertical seismic profile (VSP) in the cases of a) absence of melting, b) with melting, and c) difference.

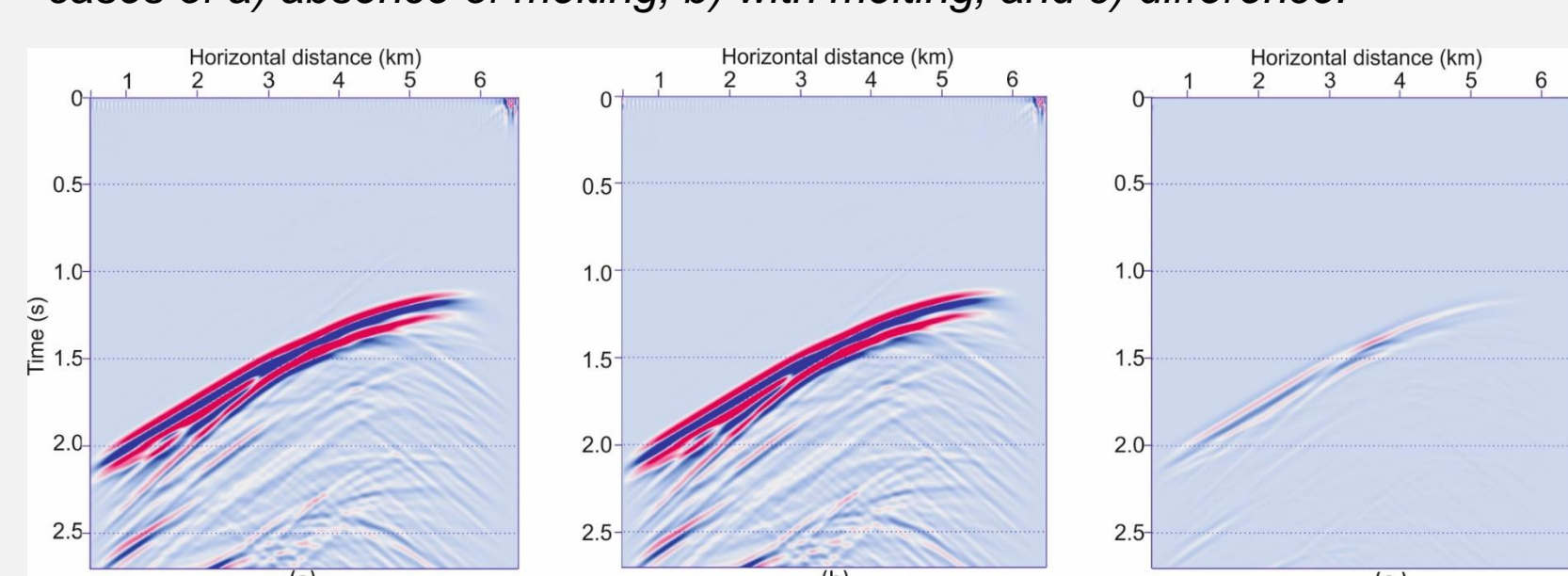


Fig. 9 Signal of the surface seismic line (vertical particle velocity) acquired a) with superhot chimneys, b) without superhot chimneys, and c) difference of the results (a) and (b).

Simulation of Acoculco EGS wavefields

The Acoculco geothermal area is located in the eastern part of the Mexican volcanic belt. The Mexican Federal Electricity Company (CFE) drilled two exploration wells EAC-1 and EAC-2, which reach a depth of 2000 m and 1900 m, respectively. The temperatures measured in the wells are around 300 °C, their linear profile is indicative of a conductive thermal regime (López-Hernández et al., 2009).

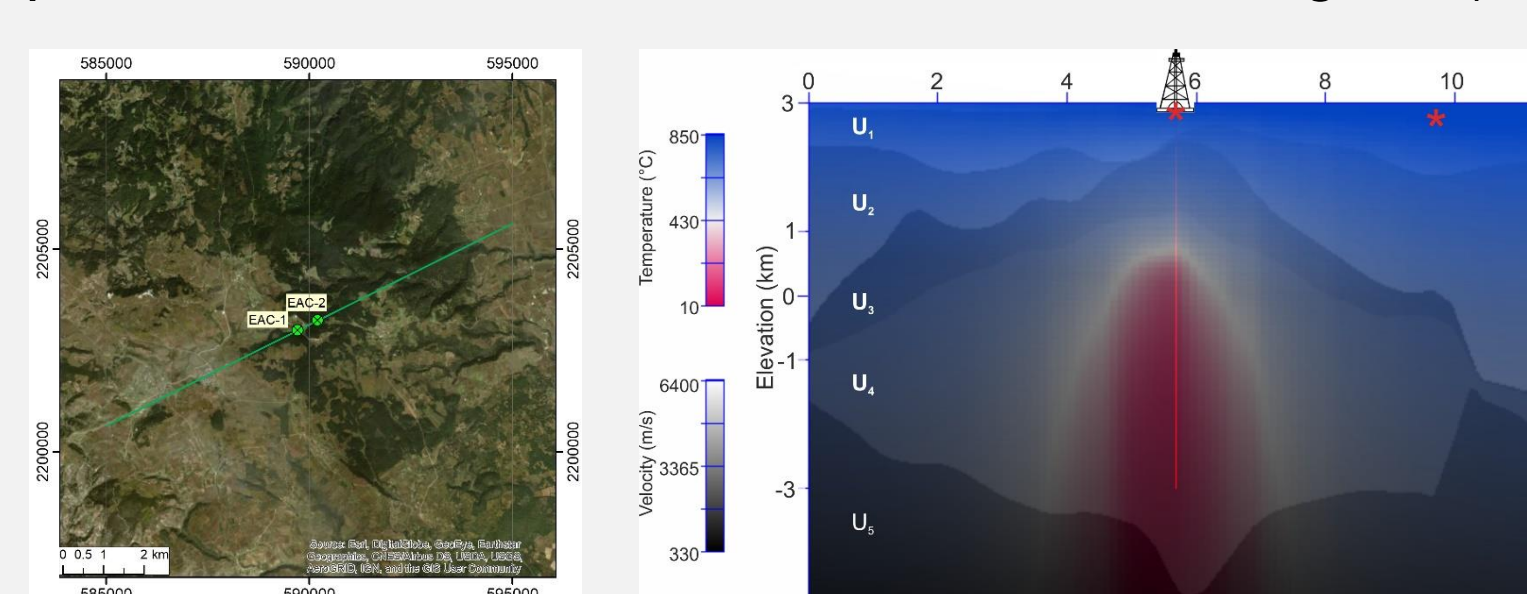


Fig. 10 Map with the position of the wells and the 2D model line.

Lithological units	Vp (km/s)	Vs (km/s)	ρ (g/cm ³)	Φ (%)	A (MPa) ⁿ s ⁻¹	n	E (kJ/mol)
U1: Volcanics	3.0	1.68	2.3	11.2	10^{-2}	1.8	151
U2: Limestone	4.8	2.7	2.6	1.17	3.3×10^{-6}	2.4	134
U3: Skarns	6.05	3.4	2.8	1.22	3.3×10^{-4}	3.2	238
U4: Granites	5.8	3.25	2.7	2	AC1) 2×10^{-4} AC2) 10^2	1.9 2.0	137 134
U5: Basement	6.4	3.6	2.9	6	6.1×10^8	3.6	456

Tab. 1 Seismic and thermodynamic (Arrhenius) parameters used to model the 2D line of Fig. 10.

We consider a 2D model along a line (Fig. 10), which crosses the two wells in the SW-NE direction. We extract the geological and temperature 2D slices (Fig. 11) from the 3D model proposed by WP3 (GEMex Deliverable D3.4, Bonté et al., 2019). In the absence of additional local information, we associated geophysical and thermal properties (Tab. 1) derived from literature. For the unit U4, which represents the crust involved in thermal anomalies, we consider two sets of Arrhenius parameters: AC1 characteristic of the upper crust (Fernández and Ranalli, 1997) and AC2 (Carcione et al., 2014). The latter characterizes a rock that melts at temperature around 700 °C (Tab. 1).

In Figs. 12 and 13 we show synthetic simulations of ideal VSP profiles, with sources at 0 and 4 km offset (red stars in Fig. 11), acquired in well EAC-2 entering the formations with and without melting conditions at the assumed temperature model.

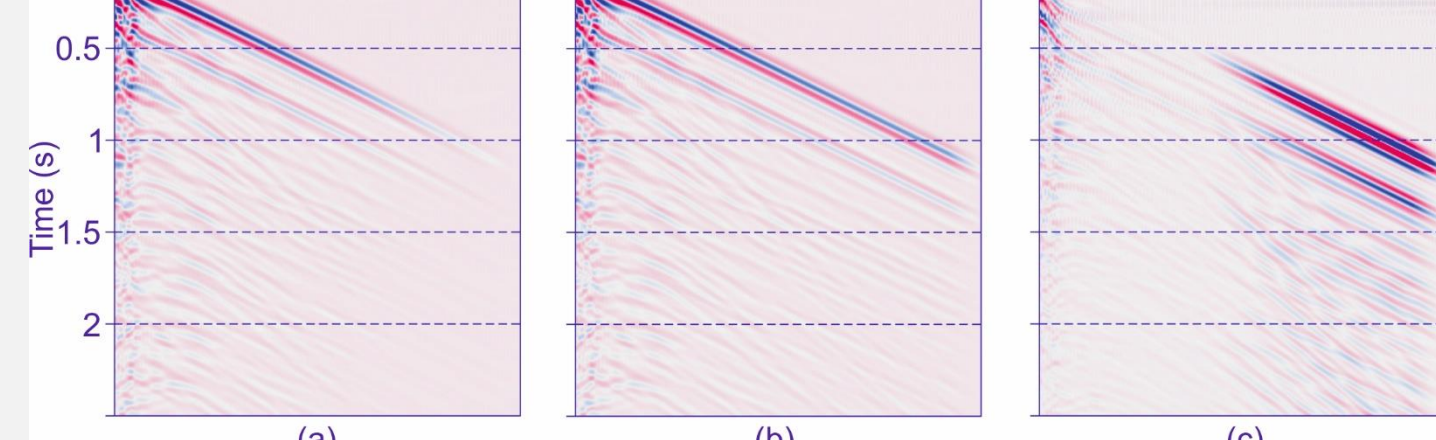


Fig. 12 VSP (vertical particle velocity) at offset 0 a) with melting, b) without melting, c) difference.

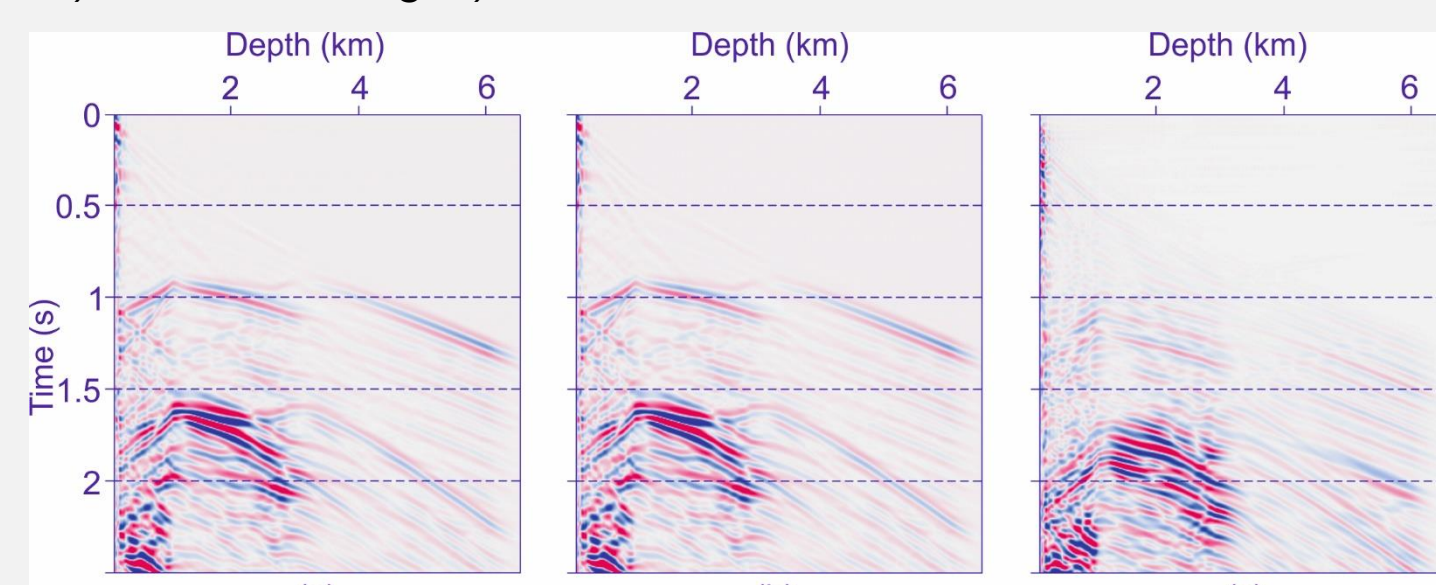


Fig. 13 VSP (vertical particle velocity) at offset 4 km a) with melting, b) without melting, c) difference.

References

- Bonté D., Limberger J., Trumpy E., Gola G., and Diederik van Wees J., 2019. D3.4: Regional resource assessment and geothermal models. Version 1, Work package 3, Website: <http://www.gemex-h2020.eu>
- Carcione J. M., Poletto F., Farina B. and Craglietto A., 2017. The Gassmann-Burgers model to simulate seismic waves at the Earth crust and mantle, Pure and Applied Geophysics, 174, 849-863.
- Carcione J.M., Poletto F., Farina B. and Craglietto A., 2014. Simulation of seismic waves at the Earth crust (brittle-ductile transition) based on the Burgers model, Solid Earth, 5, 1001-1010.
- Farina, B., Poletto, F., Mendrinis, D., Carcione, J.M., Karytsas C., 2019. Seismic properties in conductive and convective hot and super-hot geothermal systems. Geothermics 82, 16–33.
- Fernández M., and Ranalli G., 1997. The role of rheology in extensional basin formation modelling. Tectonophysics, 282, 129-145.
- Gutiérrez-Negrin, L.C.A., Izquierdo-Montalvo, G., 2010. Review and update of the main features of the Los Humeros geothermal field, Mexico. In: Proceedings World Geothermal Congress. Bali, Indonesia.
- López- Hernández, A., García-Estrada, G., Aguirre-Díaz, G., González-Partida, E., Palma-Guzmán, H., Quijano-León, J.L., 2009. Hydrothermal activity in the Tulancingo-Acoculco Caldera complex, central Mexico: exploratory studies. Geothermics 38, 279–293.
- Poletto, F., Farina, B., Carcione, J.M., Böhm, G., Mendrinis, D., Jousset, Ph., Pinna, G., Barison, E., 2019a. D5.5: Report on seismic modelling. GEMex Deliverable.
- Poletto, F., Farina, B., Carcione J. M., and Pinna G., 2019b. Analysis of seismic wave propagation in geothermal reservoirs. European Geothermal Congress Den Haag, The Netherlands, 11-14 June 2019.
- Poletto F., Farina B. and Carcione J. M., 2018. Sensitivity of seismic properties to temperature variations in a geothermal reservoir, Geothermics, 76, 149–163.
- Pulido, C.L., Armenta, M.F., Silva, G.R., 2010. Characterization of the Acoculco geothermal zone as HDR system. GRC Trans. 34.
- Verma M.P., Surendra, P., Verma, B. and Sanvincente H. [1990]. Temperature field simulation with stratification model of magma chamber under Los Humeros caldera, Puebla, Mexico. Geothermics, 19 (2), 187-197.

